

# Supporting Information

## Non-Wetting Behavior of Al-Co Quasicrystalline Approximants

### Owing to their Unique Electronic Structures

Kanika Anand<sup>1,2</sup>, Vincent Fournée<sup>1</sup>, Geoffroy Prévot<sup>3</sup>, Julian Ledieu<sup>1</sup>, Émilie Gaudry<sup>1\*</sup>

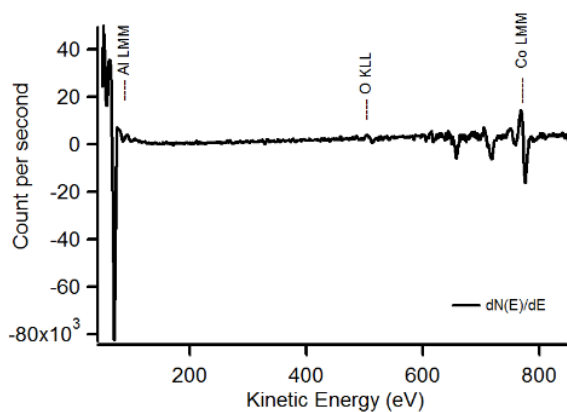
<sup>1</sup> *Université de Lorraine, CNRS, IJL, F-54000 Nancy, France*

<sup>2</sup> *CIRIMAT, Université de Toulouse, CNRS, INPT, UPS, 4 Allée Emile Monso, BP44362, 31030 Toulouse Cedex 4, France*

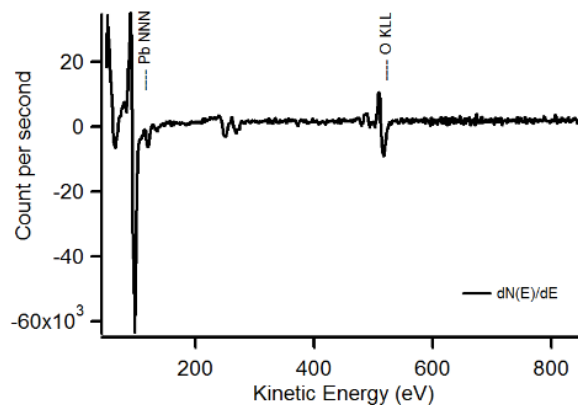
<sup>3</sup> *Sorbonne Université, CNRS, Institut des NanoSciences de Paris, 4 place Jussieu, 75005 Paris, France*

E-mail: [emilie.gaudry@univ-lorraine.fr](mailto:emilie.gaudry@univ-lorraine.fr)

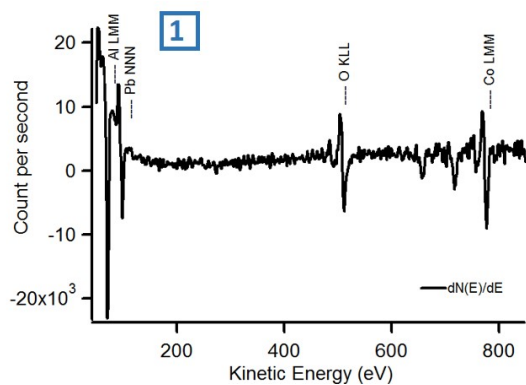
# Auger Spectra



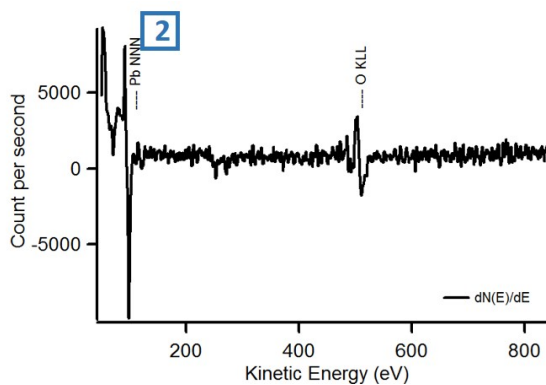
(a)



(b)



(c)



(d)

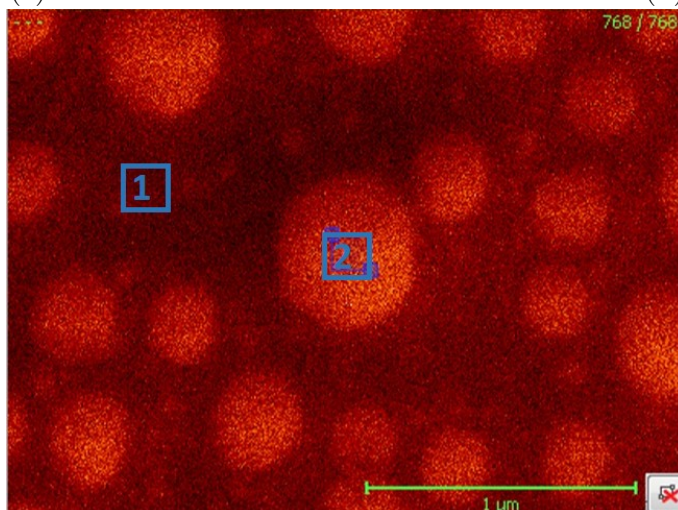


Figure S1: Top: Auger spectra of the clean  $\text{Al}_5\text{Co}_2(001)$  surface (a), of the Pb film before dewetting (b) and after dewetting (c,d). Bottom: SEM image after dewetting.

# Contact Angle Measurements

Contact angles were measured as schematically described in Fig. 2. We calculated the average contact angle ( $\theta_{avg}$ , Fig. S2), i.e. the average of the apparent angle values ( $\theta_{app}$ ) and the fitted angle values ( $\theta_{fit}$ , determined from curve-fitting) to avoid any errors due to local distortions or errors subjective to points chosen for curve fitting.<sup>1</sup> The average contact angle values were found to be independent of the droplet size as well as of the tilt angle.

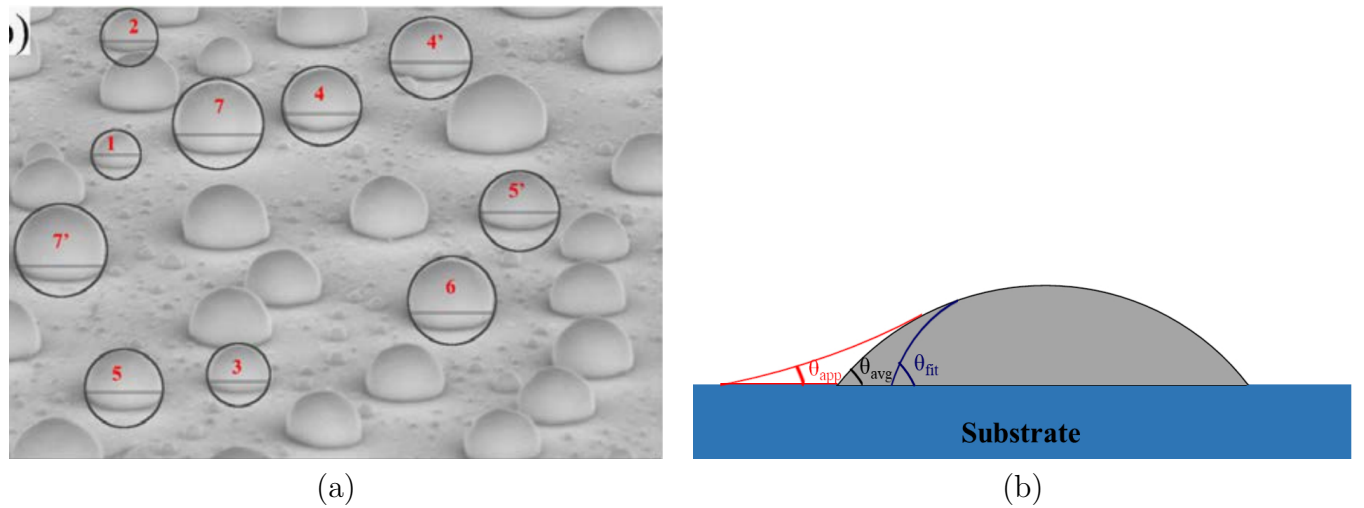


Figure S2: (a) SEM micrograph showing Pb droplets on  $\text{Al}_5\text{Co}_2(001)$ . A few droplets are curve-fitted (black circles) for contact angle measurements. The red labels are used to identify the droplets of Tab. S1. (b) Schematic representation of the different contact angles mentioned in the text.

Table S1: Contact angle measurement for Pb/ $\text{Al}_5\text{Co}_2(001)$ .

Droplet size ( $\mu\text{m}$ )		Contact angles (degrees)		
		$\theta_{fit}$	$\theta_{app}$	$\theta_{avg}$
1	1.36	98.6	85.4	92
2	1.62	101.3	86.3	93.8
3	1.78	101.8	85.9	93.85
4	2.04	102.8	86.7	94.75
5	2.29	103.3	88.5	95.56
6	2.38	108.9	89.8	99.35
7	2.41	109.1	89.6	99.5

# Surface Energy Calculations

According to Ref.,<sup>2</sup> the surface energy  $\gamma_{clean}$  of an elemental metal can be calculated using the following method. We consider a solid with a finite number  $n$  of infinitely extended planar atomic layers, and a slab of finite area  $A$  embedded in this solid. The slab has  $n$  layers, each with  $N_\ell$  atoms. The surface energy is given by

$$\gamma_{clean} = \lim_{n \rightarrow \infty} \frac{E_{slab(n)} - nN_\ell E_{bulk}}{2A} \quad (1)$$

where  $E_{slab(n)}$  is the total energy of the slab and  $E_{bulk}$  is the energy per atom of the infinite bulk. The factor of  $\frac{1}{2}$  in this equation comes from the fact that the slab is bounded by two symmetric surfaces.

In the case of compounds, the stoichiometry of the slab is in general different from the one of the bulk. The surface energy is then determined as a function of the chemical potentials.<sup>3</sup> The chemical potential of species  $i$  ( $\mu_i$ ) is defined as the derivative of the Gibbs free enthalpy  $G$  for a given phase with respect to the number of particles  $i$  and fixed numbers of other particles  $\{N_j\}$  apart from  $N_i$ :

$$\mu_i = \left( \frac{\partial G}{\partial N_i} \right)_{P,T,N_j} \quad (2)$$

For condensed states, the Gibbs free enthalpy per particle can be taken as the total energy per atom calculated at  $T = 0$  K, i.e. as the cohesive energy ( $E_{coh}$  = the energy required to separate the elements into neutral atoms at  $T = 0$  K and atmospheric pressure  $P$ ). Indeed, the Gibbs free enthalpy  $G(T, P, N)$  can be expressed using the Helmholtz free energy  $F(T, V, N)$ :  $G(T, P, N) = F(T, V, N) + PV$ . Under normal pressure ( $\simeq 1$  atm), the difference between the Helmholtz free energy  $F$  and the Gibbs free energy  $G$  ( $F - G = -PV$ ) is almost zero for a solid. In addition, the temperature-dependent term is assumed to be negligible, based on the argument that there is a partial cancellation of the  $TS$  term ( $S$  is the entropy) with the contributions of the lattice vibrations to the internal energies ( $3k_B T \sum N_i$ ), at least in the limit of the validity of the equipartition theorem.

In the case of a simple metal, the previous statements imply that the chemical potential is simply given by the cohesive energy. For example, the chemical potential for Al in bulk Al is  $\mu_{\text{Al}}^{\text{bulk}} = E_{\text{coh}}^{\text{Al}}$ . In the case of a compound, the chemical potential is given by the Gibbs phase rule (equilibrium conditions). For  $\text{Al}_x\text{Co}_y$ , it implies that :  $(x + y)\mu_{\text{Al}_x\text{Co}_y}^{\text{bulk}} = x\mu_{\text{Al}} + y\mu_{\text{Co}}$  where  $\mu_{\text{Al}}$  and  $\mu_{\text{Co}}$  are the chemical potentials of Al and Co in  $\text{Al}_x\text{Co}_y$ .

When compound surfaces are modeled with symmetric slabs, the surface energies are given by

$$\gamma_{\text{clean}} = \lim_{\text{slab}} \frac{E(N_i) - \sum N_i \mu_i}{2A} \quad (3)$$

where  $\mu_i$  and  $N_i$  are the chemical potentials and number of atoms of type  $i$  in the slab. In the previous equation, the numerator can be understood as the difference between the total energy of the slab and the energy of the corresponding bulk with the same stoichiometry.

# Bulk, Surfaces and Interfaces: Thermodynamic Results

Table S2: Cell parameters, cohesive energies and (111) surface energies of Al and Pb metals.

	$a$ (Å)	$E_{coh}$ (eV/at.)	$\gamma_{(111)}$ (meV/Å <sup>2</sup> )	
Al	4.04	-3.50	50.1	calc.
Al	4.04 <sup>4</sup>	-3.43 <sup>4</sup>	55.5 <sup>2</sup>	calc.
Al	4.04 <sup>5</sup>	-3.39 <sup>6</sup>	71.1 <sup>7</sup>	exp.
Pb	5.03	-2.94	17.8	calc.
Pb	5.05 <sup>4</sup>	-2.92 <sup>4</sup>	17.2 <sup>8</sup>	calc.
Pb	4.95 <sup>5</sup>	-2.03 <sup>9</sup>	27.5 <sup>10</sup>	exp.

Table S3: Surface structures and energies (meV/Å<sup>2</sup>, calculated with  $\mu_{Al} = \mu_{Al}^{bulk}$ ) for pristine surfaces considered in this work. The labels are those used in previous references. According to Ref.,<sup>13</sup> two models ( $P_{B-4Co}$  and  $P_B$ ) are conceivable for Al<sub>5</sub>Co<sub>2</sub>(2 $\bar{1}$ 0). The comparison between experimental and simulated STM images does not allow any discrimination between these two models, which differ by the number of protruding surface Co atoms. In this work, we built a surface model which locally presents at the surface the atomic arrangements of both  $P_{B-4Co}$  and  $P_B$  models.

Surface	Al <sub>13</sub> Co <sub>4</sub> (100)		Al <sub>5</sub> Co <sub>2</sub> (001)	Al <sub>5</sub> Co <sub>2</sub> (2 $\bar{1}$ 0)	
Surface cell	(1×1)		( $\sqrt{3} \times \sqrt{3}$ )R30 <sup>o</sup>	(2×1)	
Model	$P_{24}^{Al,Co^-}$ (Ref. <sup>11</sup> )	$P_{22}^{Al}$ (Ref. <sup>11</sup> )	$P_{6\text{ Al miss}}^{\sqrt{3} \times \sqrt{3} R30^o}$ (Ref. <sup>12</sup> )	$P_{B-4Co}$ (Ref. <sup>12</sup> )	$\langle P_{B-4Co}, P_B \rangle$
Our work	68.1	65.6	83.8	78.6	87.6
Refs.	68.0 <sup>11</sup>		83.6 <sup>12</sup>	79.3 <sup>12</sup>	

Table S4: Interfacial and modified surface energies (meV/Å<sup>2</sup>) for Pb/Al<sub>13</sub>Co<sub>4</sub>(100) models considered in this work.

	hexagonal-like	pseudomorphic-like	MD-like
$\gamma_{\text{substrate modified interface}}$	40.9	40.6	36.7
$\gamma_1^{\text{interface}}$	23.1	38.1	18.9
$\gamma_4^{\text{interface}}$	42.3	38.0	44.5

Table S5: Interfacial energies ( $\text{meV}/\text{\AA}^2$ ) for  $\text{Pb}/\text{Al}_5\text{Co}_2(2\bar{1}0)$  ( $P_{B-4Co}$  model).

Pb-adlayer thickness	$\gamma^{\text{interface}}$	$\theta$
1	36.0	
2	52.7	86
3	51.3	82
4	47.1	68

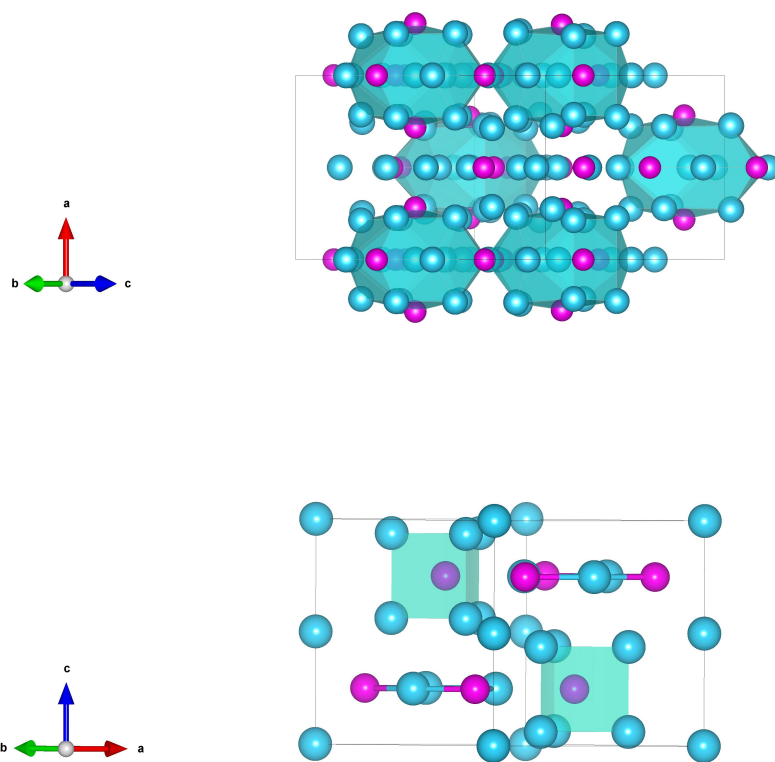


Figure S3: Bulk structures of  $\text{Al}_{13}\text{Co}_4$  (top) and  $\text{Al}_5\text{Co}_2$  (bottom). Color code: Al=blue; Co=magenta.

## Pb(111)/Al(111) : DOS and STM Images

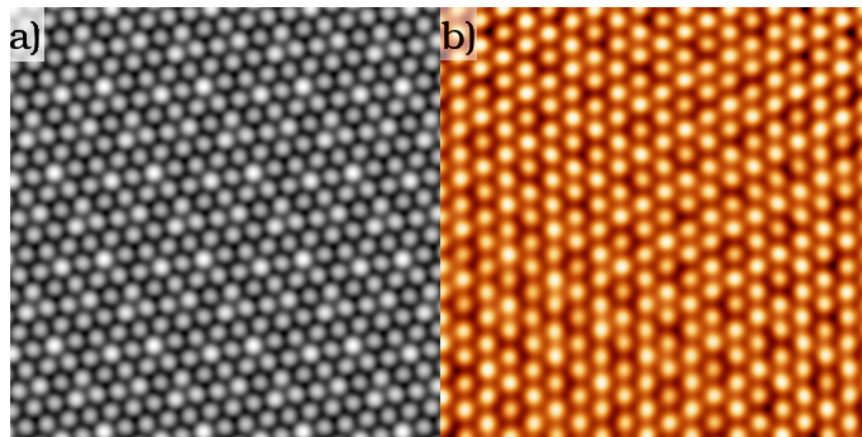


Figure S4: Theoretical (a) and Fourier filtered experimental (b) STM images ( $V_{bias} = -0.5$  eV,  $6 \times 6$  nm<sup>2</sup>) for a lead monolayer over Al(111).

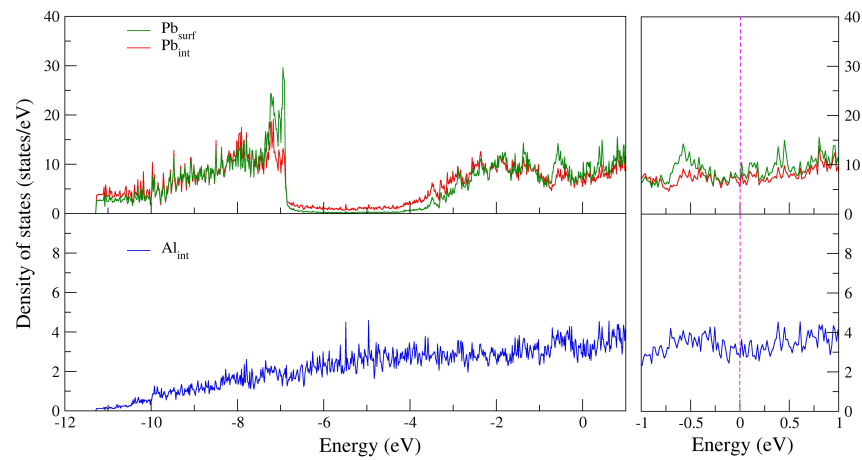


Figure S5: DOS for Pb(111)/Al(111). The considered system is built with 2 Pb-adlayers over the Al(111) substrate. The contributions of the Pb interfacial layer and the topmost Pb layer are shown in red and green, respectively. The contribution of the interfacial Al layer is shown in blue.

# Bader Charges

Table S6: Bader charges  $\Delta Q_x$  carried by interfacial atoms. The value is averaged over the atoms of the considered layer.

System	Nb	Pb <sub>int</sub>	Al <sub>int</sub>	Al <sub>int-1</sub>	Co <sub>int-1</sub>
Pb(111)/Al(111)	1	-0.04	0.02	0.02	-
Pb(111)/Al(111)	2	-0.04	0.02	0.00	-
Pb(111)/Al(111)	3	-0.04	0.02	0.01	-
Pb(111)/Al(111)	4	-0.05	0.02	0.01	-
Al <sub>13</sub> Co <sub>4</sub> (100)			0.23 ± 0.08	0.94 ± 0.10	-3.26 ± 0.20
Pb(111)/Al <sub>13</sub> Co <sub>4</sub> (100)	1	-0.06	0.36	1.00	-3.42
Pb(111)/Al <sub>13</sub> Co <sub>4</sub> (100)	2	-0.08	0.27	1.00	-3.33
Pb(111)/Al <sub>13</sub> Co <sub>4</sub> (100)	3	-0.06	0.32	1.00	-3.43
Pb(111)/Al <sub>13</sub> Co <sub>4</sub> (100)	4	-0.10	0.30	1.00	-3.37
Al <sub>5</sub> Co <sub>2</sub> (001)			0.67 ± 0.20	1.24 ± 0.05	-2.92 ± 0.45
Pb(111)/Al <sub>5</sub> Co <sub>2</sub> (001)	1	-0.06	0.76	1.25	-3.05
Pb(111)/Al <sub>5</sub> Co <sub>2</sub> (001)	2	-0.08	0.76	1.27	-3.02
Pb(111)/Al <sub>5</sub> Co <sub>2</sub> (001)	3	-0.06	0.74	1.26	-3.02
Pb(111)/Al <sub>5</sub> Co <sub>2</sub> (001)	4	-0.10	0.76	1.26	-3.01

## References

1. Kaplan, W.; Chatain, D.; Wynblatt, P.; Carter, W. C. A Review of Wetting Versus Adsorption, Complexions, and Related Phenomena: the Rosetta Stone of Wetting. *J. Mater. Sci.* **2013**, *48*, 5681–5717.
2. Patra, A.; Bates, J. E.; Sun, J.; Perdew, J. P. Properties of Real Metallic Surfaces: Effects of Density Functional Semilocality and Van der Waals Nonlocality. *PNAS* **2017**, *114*, E91.
3. Bechstedt, F. *Principles of Surface Physics*; Springer: Berlin, 2003.
4. Lejaeghere, K.; Speybroeck, V. V.; Oost, G. V.; Cottenier, S. Error Estimates for Solid-State Density-Functional Theory Predictions: an Overview by Means of the Ground-

- State Elemental Crystals. *Critical Reviews in Solid State and Materials Sciences* **2014**, *39*, 1–24.
5. Villars, P.; Cenzual, K. *Pearsons Crystal Data - Crystal Structure Database for Inorganic Compounds, Release 2012/13*; Materials Park, Ohio, USA: ASM International, 2013.
  6. Boer, F. D.; Boom, R.; Mattens, W.; Miedema, A.; Niessen, A. *Cohesion in Metals*; Elsevier, Amsterdam, 1988.
  7. Tyson, W.; Miller, W. Surface free energies of solid metals: Estimation from Liquid Surface Tension Measurements. *Surf. Sci.* **1977**, *62*, 267.
  8. Yu, D.; Scheffler, M. First-Principles Study of Low-Index Surfaces of Lead. *Phys. Rev. B* **2004**, *70*, 155417 (1to9).
  9. Kittel, C. *Introduction to Solid State Physics*, 7th ed.; John Wiley & Sons: USA, 1996.
  10. Bombis, C.; Emundts, A.; Nowicki, M.; Bonzel, H. Absolute Surface Free Energies of Pb. *Surface Science* **2002**, *511*, 83–96.
  11. Gaudry, E.; Chatelier, C.; McGuirk, G.; Loli, L. S.; DeWeerd, M.-C.; Ledieu, J.; Fournée, V.; Felici, R.; Drnec, J.; Beutier, G. *et al.* Structure of the Al<sub>13</sub>Co<sub>4</sub>(100) Surface: Combination of Surface X-Ray Diffraction and Ab Initio Calculations. *Phys. Rev. B* **2016**, *94*, 165406.
  12. Meier, M.; Ledieu, J.; Fournée, V.; Gaudry, E. Semi-Hydrogenation of Acetylene On Al<sub>5</sub>Co<sub>2</sub> Surfaces. *J. Phys. Chem. C* **2017**, *121*, 4958–4969.
  13. Meier, M.; Ledieu, J.; Weerd, M.-C. D.; Huang, Y.-T.; Abreu, G. J. P.; Diehl, R.; Mazet, T.; Vincent.Fournée,; Gaudry, E. Interplay Between Bulk Atomic Clusters and Surface Structure in Complex Intermetallic Compounds: the Case Study of the Al<sub>5</sub>Co<sub>2</sub>(001) Surface. *Phys. Rev. B* **2015**, *91*, 085414 (1to16).